iScience

CellPress
OPEN ACCESS

Article

The biological effects of terahertz wave radiation-induced injury on neural stem cells

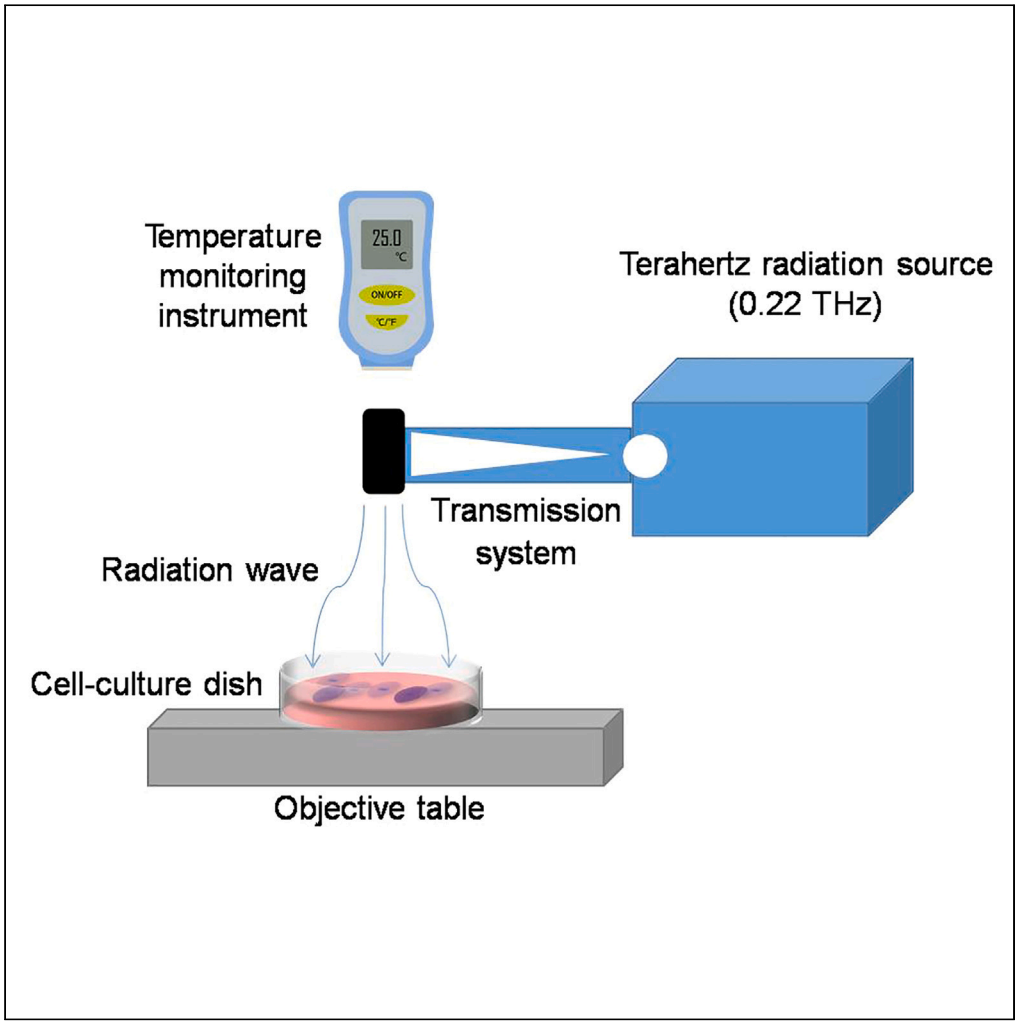

Yunxia Wang, Yu Xiong, Man Chen, ..., Peng Gao, Guiming Xiang, Liqun Zhang

1434103777@qq.com

Highlights

Terahertz (THz) radiation has biological effects on neural stem cells (NSCs)

Compared to mouse NSCs, human NSCs were more vulnerable to damage

The proliferation and apoptosis of NSCs were dose-dependently affected by THz irradiation

Wang et al., iScience *26*, 107418
October 20, 2023 © 2023
https://doi.org/10.1016/j.isci.2023.107418

iScience

CellPress
OPEN ACCESS

Article

The biological effects of terahertz wave radiation-induced injury on neural stem cells

Yunxia Wang,[1] Yu Xiong,[1] Man Chen,[2] Fei Liu,[2] Haiyan He,[1] Qinlong Ma,[3] Peng Gao,[3] Guiming Xiang,[2] and Liqun Zhang[2,4,*]

SUMMARY

Terahertz (THz) is an electromagnetic wave with a radiation wavelength range of 30–3000 μm and a frequency of 0.1–10 THz. With the development of new THz sources and devices, THz has been widely applied in various fields. However, there are few studies on biological effects of THz irradiation on the human neural stem cells (hNSCs) and mouse neural stem cells (mNSCs), which need to be further studied. We studied the biological effects of THz radiation on hNSCs and mNSCs. The effects of THz irradiation time and average output power on the proliferation, apoptosis, and DNA damage of NSCs were analyzed by flow cytometry and immunofluorescence. The results showed that the proliferation and apoptosis of NSCs were dose-dependently affected by THz irradiation time and average output power. The proliferation of hNSCs was more vulnerable to damage and apoptosis was more serious under the same terahertz irradiation conditions compared to those of mNSCs.

INTRODUCTION

A terahertz (THz) wave has a special frequency band in the entire electromagnetic spectrum; it is an electromagnetic wave with a radiation wavelength range of 30–3000 μm and a frequency of 0.1–10 THz.[1–3] In recent years, with the vigorous development of a variety of new THz sources and devices, it has been widely applied in various fields, including biology,[4] medicine,[5,6] military and security checks,[7–9] counterterrorism,[10] material structure detection,[11] communication,[12] remote sensing radar,[13] and data transmission.[14] In military affairs and security inspection, THz technology should be used for noncontact scanning and detection of hidden dangerous products, drugs, and weapons.[15] In biomedicine, THz radiation has low quantum energy and theoretically does not cause tissue ionization, so it can be used in biological sample examination,[16,17] identification of biological macromolecules and small molecules,[18–21] and biological information extraction.[22] However, the safe range for the intensity and duration of terahertz irradiation remains to be further investigated, and the biological safety of THz has received increasing attention, especially in safety inspections. Research on THz biological effects is the basis and premise for evaluating the safety of THz in organisms. Therefore, investigating the effects of THz radiation on cells for the wider application of THz technology is extremely important in the future.

Numerous studies have shown that THz radiation can alter the physiological state of cells, including the cell stress response, cell proliferation,[23] and other biological functions.[24] Abnormal assembly of spindle proteins and chromosomal mis-segregation caused by THz irradiation were observed in human fetal fibroblasts.[25] Moreover, Hintzsche et al. suggested that THz radiation is a spindle-acting agent, as predominantly indicated by the appearance of spindle disturbances at anaphase and telophase (especially lagging and nondisjunction of single chromosomes) of cell divisions.[26] Moreover, Titova et al. observed that exposure to intense THz pulses for 10 min leads to a significant induction of H2AX phosphorylation, indicating that THz pulse irradiation may cause DNA damage in exposed skin tissue.[27] Cherkasova et al. also found that human lymphocytes exposed to THz showed increased cell death.[28] Borovkava et al. revealed that when rat glial cells were exposed to THz for 1 min, the apoptosis rate of cells increased 1.5 times, and when they were exposed to THz for 3 min, the apoptosis of cells increased 2 times. This effect was positively correlated with the irradiation time.[29] In addition, the death of fibroblasts was observed after only 12 s of exposure.[30] Furthermore, stem cells are extremely sensitive to environmental changes. Thus, these cells can be considered a favorable model for exploring the effects of biological systems exposure to THz waves. In recent years, an increasing number of studies have revealed that THz irradiation is also an important

[1]Department of Laboratory Medicine, Southwest Hospital, Army Medical University, Chongqing 400038, China

[2]Department of Clinical Laboratory, The Second Affiliated Hospital, Army Medical University, Chongqing 400037, China

[3]Department of Occupational Health, Faculty of Preventive Medicine, Key Laboratory of Electromagnetic Radiation Protection, Ministry of Education of China, Army Medical University, Chongqing 400038, China

[4]Lead contact

*Correspondence: 1434103777@qq.com

https://doi.org/10.1016/j.isci.2023.107418

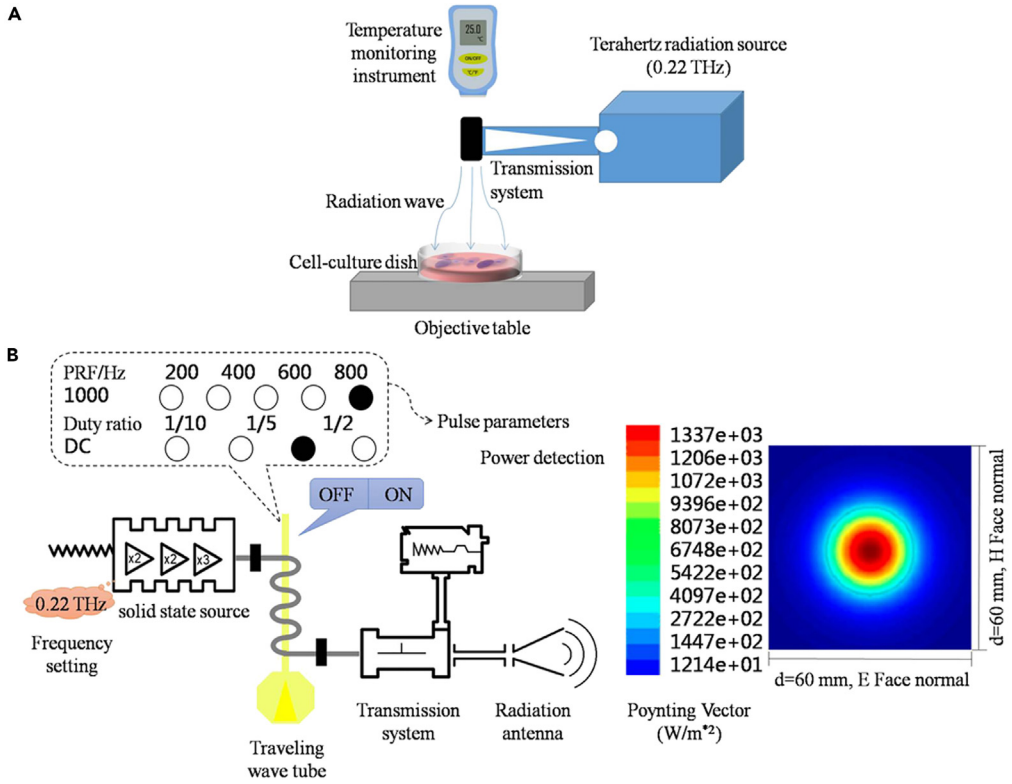

Figure 1. Schematics of THz wave radiation

(A) the components of the THz irradiation device, and (B) the parameter setting platform.

cause of changes in stem cell physiological function. Exposure to THz irradiation was shown to cause changes in the gene expression of human embryonic stem cells, and whole genome analysis showed that the genes with abnormal expression mainly encode THz-sensitive proteins.[31] Moreover, aberrant gene expression induced by THz irradiation has been found in human induced pluripotent stem cells.[32] THz irradiation also resulted in abnormal gene expression in mouse stem cells.[33,34] All these results indicate that THz radiation can cause different degrees of impairment to cells. However, the effects of THz radiation on the biological functions of neural stem cells have not been reported.

To investigate the changes in neural stem cell status after a certain period of irradiation, this study used a THz source with a frequency of 0.22 THz to irradiate neural stem cells (Figure 1). Recent studies have found that THz irradiation can change the behavioral phenotype of mice to a certain extent; however, the effect of terahertz irradiation on neural stem cells in mice has not been studied.[35] Therefore, we first investigated the effects of THz irradiation on mNSCs, and we further selected hNSCs derived from iPSCs to investigate the biological effects of THz irradiation. In this study, flow cytometry was used to analyze proliferation and apoptosis in neural stem cells, and immunofluorescence was used to analyze DNA damage in neural stem cells. The results showed that THz irradiation disrupted the proliferation of neural stem cells and led to DNA damage and apoptosis. Furthermore, the proliferation of neural stem cells was negatively correlated with THz irradiation time and intensity. Moreover, the degree of DNA damage and apoptosis of neural stem cells were positively correlated with the time of THz irradiation. Interestingly, there was a dose-dependent relationship between DNA damage and THz radiation intensity in hNSCs but not in mNSCs. Overall, the proliferation of hNSCs is more susceptible to being affected and apoptosis is more serious under the same terahertz irradiation conditions.

RESULTS

THz radiation impaired mouse neural stem cell proliferation

To investigate the effects of THz irradiation on neural stem cells, we first performed experiments on mouse-derived neural stem cells (mNSCs). Here, we analyzed the effects of different irradiation time with the same

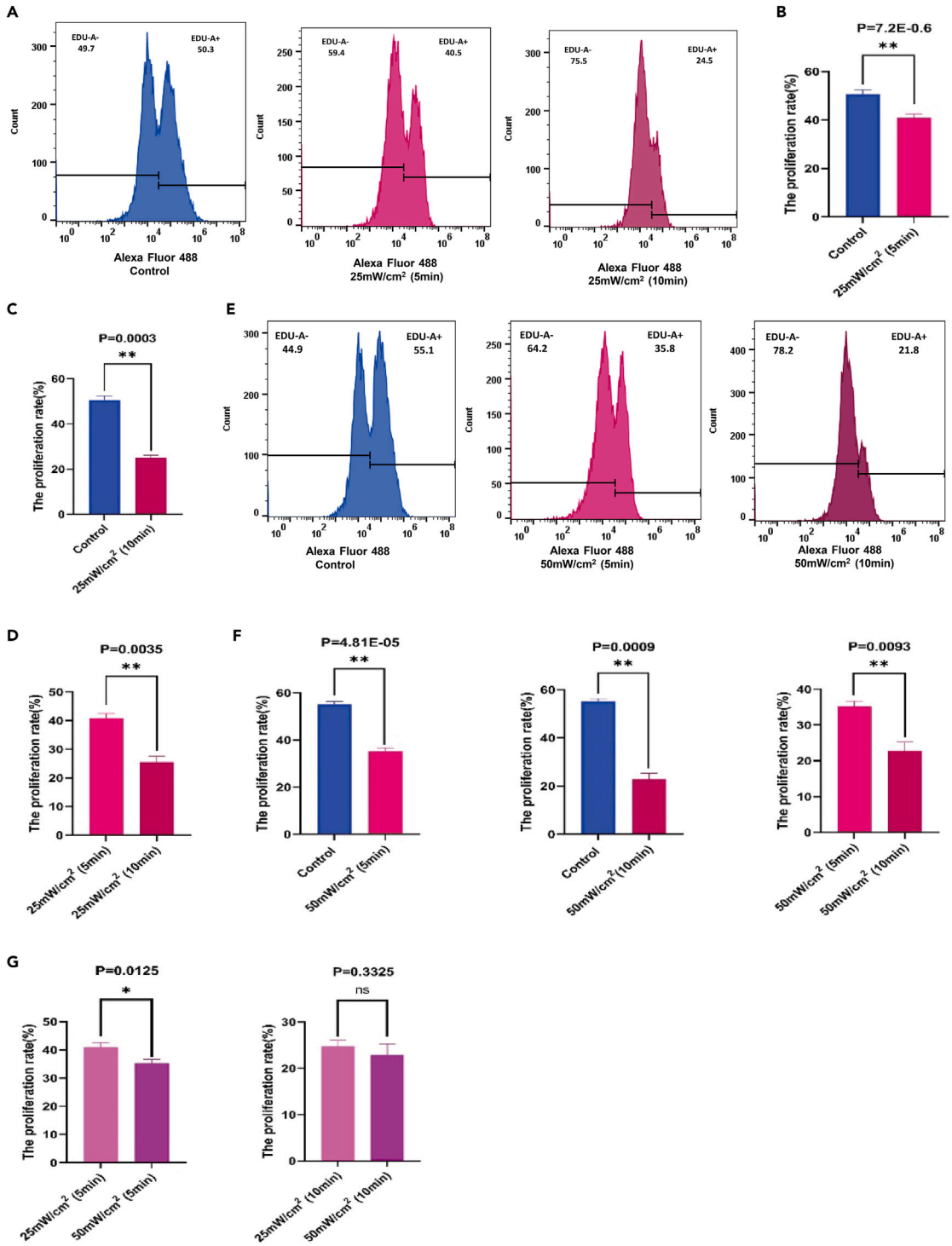

Figure 2. THz radiation impaired mouse neural stem cell proliferative capacity

(A) Representative flow cytometry analysis of mNSC proliferation with 25 mW/cm^2 THz irradiation (n = 3 samples from 3 mice, 1 sample per mouse).

(B, C, and D) Quantification of mNSC proliferation in different THz treatment time groups: 25 mW/cm^2 (5 min) and 25 mW/cm^2 (10 min). ** means $p < 0.01$.

(E) Representative flow cytometry analysis of mNSC proliferation with 50 mW/cm^2 THz irradiation (n = 3 samples from 3 mice, 1 sample per mouse).

(F) Quantification of mNSC proliferation in different THz treatment time groups: 50 mW/cm^2 (5 min) and 50 mW/cm^2 (10 min). ** means $p < 0.01$.

(G) Quantification of mNSC proliferation in different THz irradiation intensity groups: 25 mW/cm^2 (5 min) and 50 mW/cm^2 (5 min), 25 mW/cm^2 (10 min) and 50 mW/cm^2 (10 min). * means $p < 0.05$, ns means no significant difference.

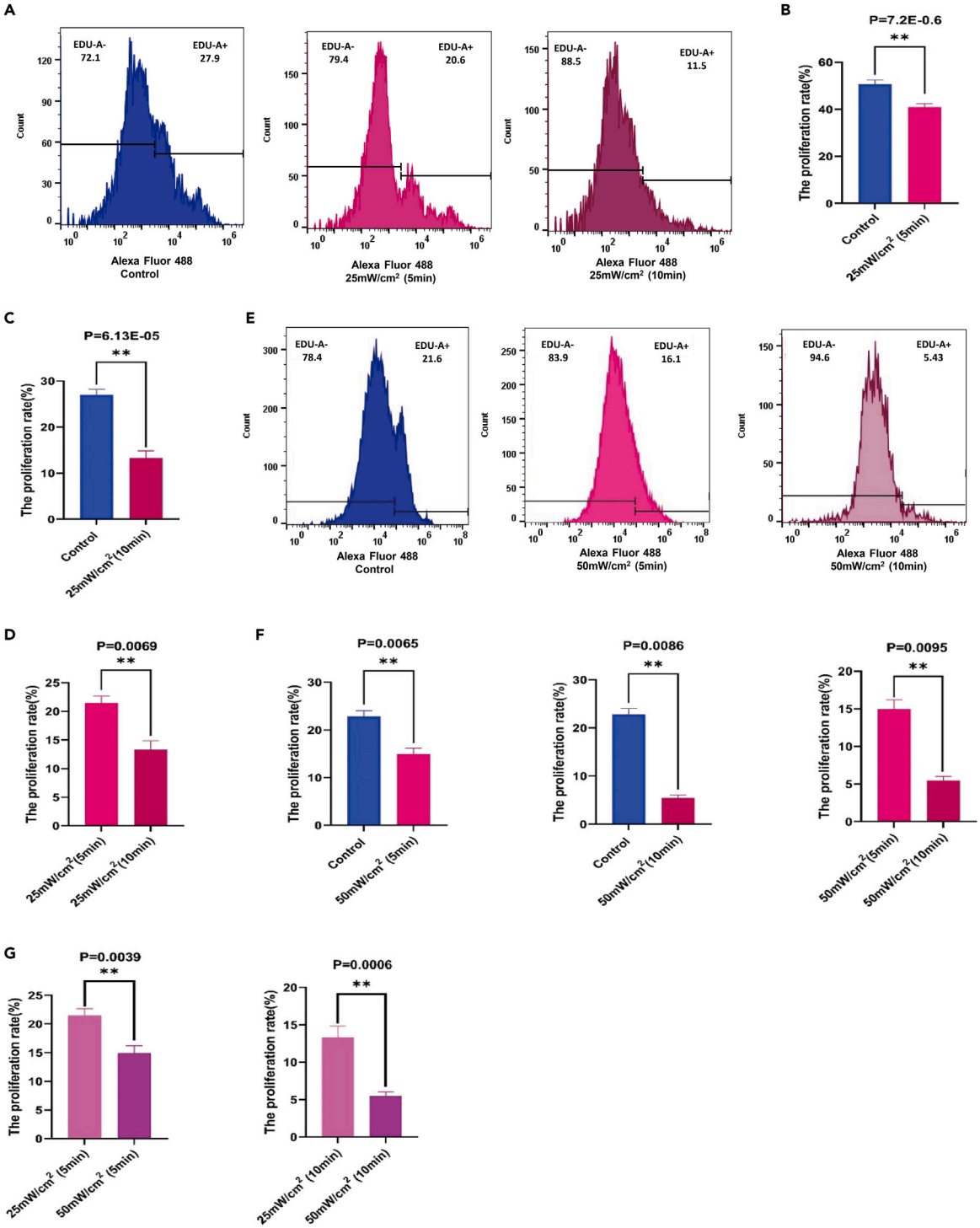

Figure 3. THz radiation impaired human neural stem cell proliferation

(A) Representative flow cytometry analysis of hNSC proliferation with 25 mW/cm^2 THz irradiation (n = 3).

(B, C, and D) Quantification of hNSC proliferation in different THz treatment time groups: 25 mW/cm^2 (5 min) and 25 mW/cm^2 (10 min). ** means $p < 0.01$.

(E) Representative flow cytometry analysis of hNSC proliferation with 50 mW/cm^2 THz irradiation (n = 3).

(F) Quantification of hNSC proliferation in different THz treatment time groups: 50 mW/cm^2 (5 min) and 50 mW/cm^2 (10 min). ** means $p < 0.01$.

(G) Quantification of hNSC proliferation in different THz irradiation intensity groups: 25 mW/cm^2 (5 min) and 50 mW/cm^2 (5 min), 25 mW/cm^2 (10 min), and 50 mW/cm^2 (10 min). ** means $p < 0.01$.

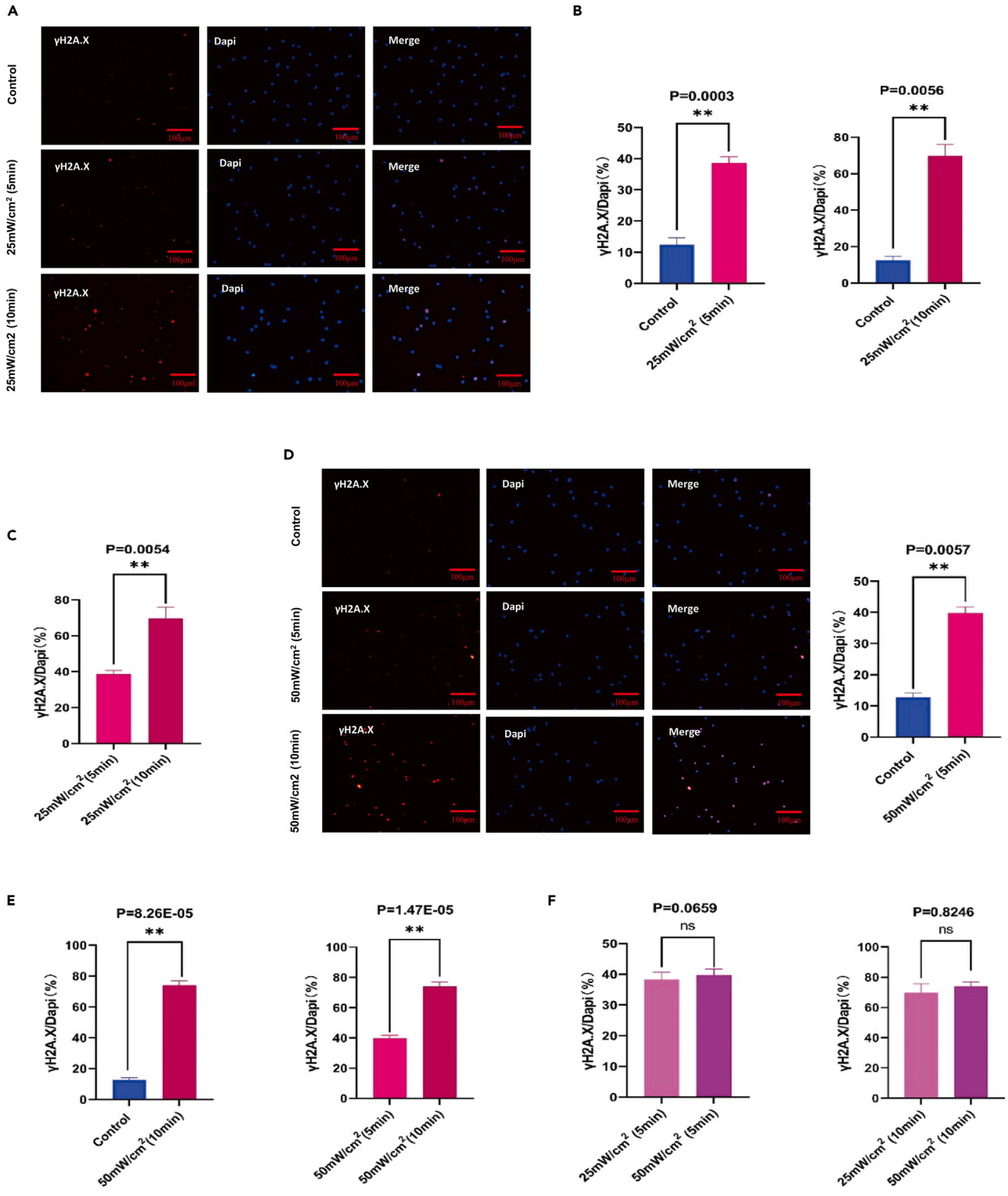

Figure 4. THz treatment disrupted DNA damage repair in mNSCs

(A) Representative immunofluorescence (IF) staining of DNA damage in mNSCs treated with 25 mW/cm^2 THz irradiation (n = 3 samples from 3 mice, 1 sample per mouse).

(B and C) Quantification of mNSC DNA damage in different THz treatment time groups: 25 mW/cm^2 (5 min) and 25 mW/cm^2 (10 min). ** means $p < 0.01$.

Figure 4. *Continued*

(D) Representative immunofluorescence (IF) staining of DNA damage in mNSCs treated with 50 mW/cm^2 THz irradiation (n = 3 samples from 3 mice, 1 sample per mouse). ** means $p < 0.01$.

(D and E) Quantification of mNSC DNA damage in different THz treatment time groups: 50 mW/cm^2 (5 min) and 50 mW/cm^2 (10 min). ** means $p < 0.01$.

(F) Quantification of mNSC DNA damage in different THz irradiation intensity groups: 25 mW/cm^2 (5 min) and 50 mW/cm^2 (5 min), 25 mW/cm^2 (10 min) and 50 mW/cm^2 (10 min). ns means no significant difference.

average output power of THz on the proliferation of mNSCs by flow cytometry (Figure 2A). When the neural stem cells were irradiated with THz radiation at the same average output power (25 mW/cm^2), the proliferation of the neural stem cells decreased with increasing irradiation time (5 min, 10 min) (Figures 2B and 2C). Moreover, doubling the THz irradiation time resulted in a significant reduction in the proliferative capacity of mNSCs (Figure 2D). Furthermore, we increased the average output power of THz to 50 mW/cm^2 (Figure 2E). The proliferation of mNSCs also decreased with increasing THz irradiation time (5 min, 10 min) (Figure 2F). Interestingly, we found that during the same irradiation time (5 min), the change in THz average output power also resulted in a significant impairment of mouse neural stem cell proliferation (Figure 2G). Notably, the average output power was increased without significantly altering the proliferation of mNSCs when THz irradiation was performed for 10 min (Figure 2G). We hypothesized that this phenomenon might be due to the proliferation of mNSCs being more sensitive to THz irradiation time. These results indicated that the degree of damage to the mNSC proliferation was dose-dependent on the THz irradiation time and power output.

THz radiation impaired human neural stem cell proliferation

Due to species differences, mNSCs cannot fully reflect the effects of THz irradiation on hNSCs. Furthermore, the effects of irradiation time on the proliferation of hNSCs were analyzed by the same method. First, as in the previous study of mNSCs, we irradiated the hNSCs with a THz source for 5 min and 10 min with an average THz output power of 25 mW/cm^2 (Figure 3A). Increasing the THz irradiation time resulted in decreased proliferation of hNSCs as before (Figures 3B, 3C, and 3D). Then, we increased the THz average output power to 50 mW/cm^2 to investigate the effect of different irradiation times on the proliferation of hNSCs (Figure 3E). We also found a negative effect of THz irradiation time on hNSC proliferation (Figure 3F). Through the analysis of different THz average output power treatment groups, we found that increasing the THz average output power would damage human neural stem cell proliferation under the same THz irradiation time, and hNSCs showed a lower proliferation rate than mNSCs (Figures 2G and 3G).

THz treatment disrupted DNA damage repair in mNSCs

To study the effects of THz treatment on the nucleic acid molecules of mNSCs, we detected markers (γH2A.X) of DNA damage by immunofluorescence; this protein is an important factor inducing cell apoptosis. The degree of DNA damage was represented by γH2A.X/DAPI. Neural stem cells were treated by THz at different average output powers and irradiation time (Figures 4A and 4D). The results indicated that the degree of DNA damage in mNSCs was positively correlated with THz irradiation time compared to that of the control group when the THz average output power was 25 mW/cm^2 (Figure 4B). The extension of THz irradiation time strongly promoted the degree of DNA damage in mNSCs (Figure 4C). To further investigate the effect of THz irradiation, we increased the THz average output power to 50 mW/cm^2 and studied the impact of different irradiation time on DNA damage (Figure 4D). The results showed that the expression of γH2A.X increased with the increasing THz irradiation time (Figures 4D and 4E). Moreover, we analyzed and compared the effect of increasing the THz average output power on DNA damage in mNSCs during the same irradiation time. Surprisingly, we found that the increase in THz power output did not further promote DNA damage in mNSCs over the same THz treatment time (Figure 4F).

THz treatment disrupted DNA damage repair in hNSCs

To gain more insight into the effect of THz irradiation on DNA damage, we studied the DNA damage of THz treatment on hNSCs by the same experimental method (Figure 5A). The results showed that when the THz average output power was set to 25 mW/cm^2, the degree of DNA damage in hNSCs became increasingly serious with the extension of irradiation time (Figures 5B and 5C). Furthermore, we changed the THz average output power to 50 mW/cm^2, and the irradiation time were 5 min and 10 min (Figure 5D). We found that the 50 mW/cm^2 THz average output power led to DNA damage in hNSCs (Figure 5D). However, the increased irradiation time did not significantly change the degree of DNA damage under the same THz average output power (Figures 5D and 5E). Simultaneously, we also found that the degree of DNA damage

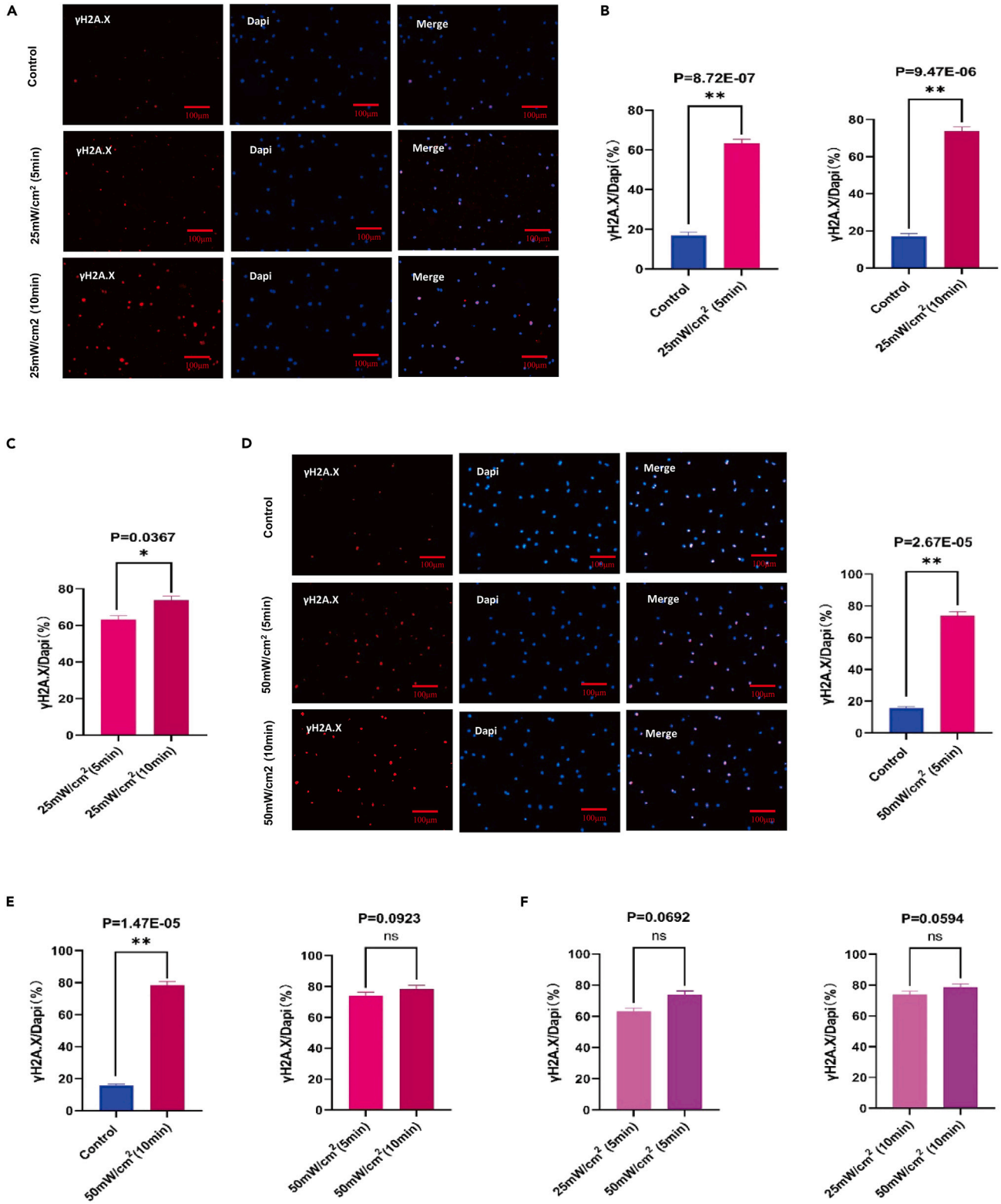

Figure 5. THz treatment disrupted DNA damage repair in hNSCs

(A) Representative immunofluorescence (IF) staining of DNA damage in hNSCs treated with 25 mW/cm^2 THz irradiation (n = 3).

Figure 5. *Continued*

(B and C) Quantification of hNSC DNA damage in different THz treatment time groups: 25 mW/cm^2 (5 min) and 25 mW/cm^2 (10 min). ** means $p < 0.01$, *means $p < 0.05$.

(D) Representative immunofluorescence (IF) staining of DNA damage in hNSCs treated with 50 mW/cm^2 THz irradiation (n = 3). ** means $p < 0.01$.

(D and E) Quantification of hNSC DNA damage in different THz treatment time groups: 50 mW/cm^2 (5 min) and 50 mW/cm^2 (10 min). ** means $p < 0.01$, ns means no significant difference.

(F) Quantification of hNSC DNA damage in different THz irradiation intensity groups: 25 mW/cm^2 (5 min) and 50 mW/cm^2 (5 min), 25 mW/cm^2 (10 min) and 50 mW/cm^2 (10 min). ns means no significant difference.

did not change significantly by comparing the relationship between DNA damage of neural stem cells and the THz output power during the same THz irradiation time (Figure 5F). Combined with the effects of THz irradiation on the degree of DNA damage in mNSCs, we conclude that hNSCs are more vulnerable to THz irradiation than mNSCs.

THz treatment-induced apoptosis of mNSCs

Apoptosis is one of the evaluation indices of neural stem cell status and reflects the physiological functions of neural stem cells. To better examine the effect of THz irradiation on neural stem cells, we performed flow cytometry with propidium iodide (PI) and fluorescein isothiocyanate (FITC) to analyze the apoptosis of mNSCs (Figure 6A). THz irradiation greatly induced acute apoptosis of neural stem cells (Figures 6B and 6C), and the apoptosis rate increased with the extension of irradiation time (Figure 6D). To further investigate the effect of irradiation time on apoptosis under different THz average output powers, we increased it to 50 mW/cm^2 (Figure 6E). The results showed that the difference in THz irradiation time was one of the causes of neural stem cell apoptosis (Figure 6F). Notably, the apoptosis rate of neural stem cells varied with THz average output power during the same irradiation time (Figure 6G). This result was different from the effects of THz on DNA damage.

THz irradiation-induced apoptosis of hNSCs

To further investigate the effect of THz irradiation on neural stem cells, we performed the same experiments with hNSCs. Then, flow cytometry was used to study the apoptosis of hNSCs (Figure 7A). When the THz average output power was 25 mW/cm^2, the apoptosis of neural stem cells increased in a time-dependent manner (Figures 7B, 7C, and 7D). Similarly, when hNSCs were treated by THz irradiation with 50 mW/cm^2 average output power (Figure 7E), we found that the apoptosis rate of human neural stem cells (hNSCs) was also increased with the extension of THz exposure time (Figure 7F). This conclusion was similar to the previous result that neural stem cell apoptosis was positively correlated with THz average output power (Figure 7G). However, compared to the mouse neural stem, the apoptosis of hNSCs was more sensitive to THz average output power and showed a higher apoptosis rate during the same THz treatment time (Figures 6G and 7H). All these results revealed that hNSCs are more sensitive to THz irradiation. The DNA of neural stem cells is more easily damaged, which leads to impaired proliferation and an increased apoptotic rate.

DISCUSSION

With the application of THz technology in the biomedical field, studying the potential effects of THz radiation on biological systems is a critical issue. The reasonable exposure levels and health consequences of THz irradiation are becoming a topic of increasing concern.[27] Our study revealed that THz irradiation with an average power of 25 mW/cm^2 and 50 mW/cm^2 resulted in proliferative disorder, abnormal DNA damage repair, and increased apoptosis of neural stem cells within the same treatment time. Simultaneously, the proliferation of neural stem cells was negatively correlated with THz irradiation intensity and irradiation time, while the DNA damage and apoptosis of neural stem cells were positively correlated with THz intensity and irradiation time. However, the tolerance of proliferation, DNA damage and apoptosis in hNSCs to THz irradiation is different from that of mNSCs.

The effects of THz on different cell types have been studied extensively. Cherkasova et al. reported the effects of THz irradiation on erythrocytes and found that THz irradiation promoted the release of hemoglobin from erythrocytes.[28] Under certain conditions in which cells are exposed to THz radiation, signs of direct DNA damage appear.[36] Kovalevska et al. showed an increased death rate of primary human mononuclear blood cells (monocytes and B-and T cells) upon 0.14 THz irradiation.[37]

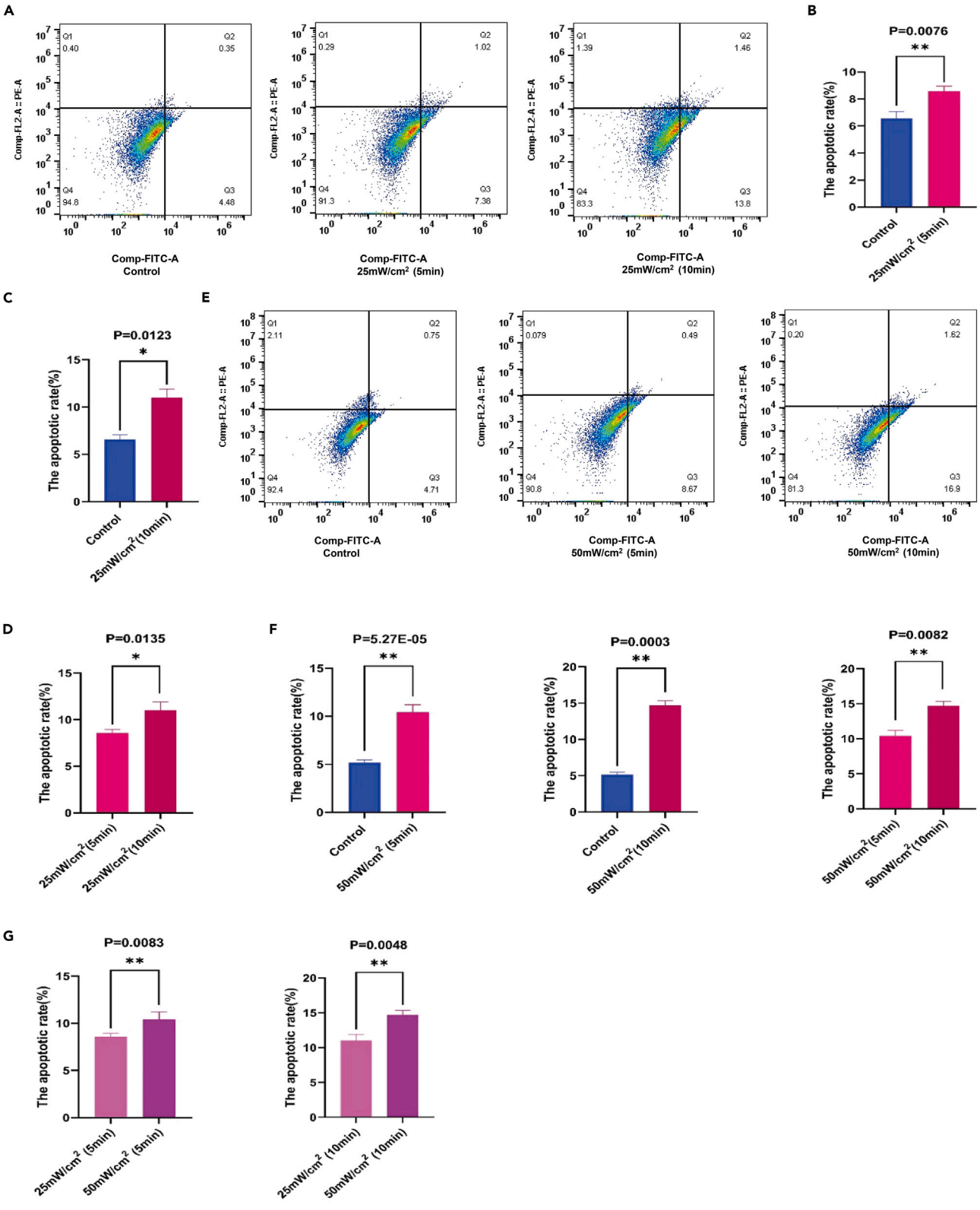
A
Q1 0.40
Q2 0.35
Q4 94.8
Q3 4.48
Comp-FL2-A :: PE-A
Comp-FITC-A
Control
Q1 0.29
Q2 1.02
Q4 91.3
Q3 7.38
Comp-FITC-A
25mW/cm² (5min)
Q1 1.39
Q2 1.46
Q4 83.3
Q3 13.8
Comp-FITC-A
25mW/cm² (10min)
B
P=0.0076
**
The apoptotic rate(%)
Control
25mW/cm² (5min)
C
P=0.0123
*
The apoptotic rate(%)
Control
25mW/cm²(10min)
E
Q1 2.11
Q2 0.75
Q4 92.4
Q3 4.71
Comp-FITC-A
Control
Q1 0.079
Q2 0.49
Q4 90.8
Q3 8.67
Comp-FITC-A
50mW/cm² (5min)
Q1 0.20
Q2 1.62
Q4 81.3
Q3 16.9
Comp-FITC-A
50mW/cm² (10min)
D
P=0.0135
*
The apoptotic rate(%)
25mW/cm²(5min)
25mW/cm²(10min)
F
P=5.27E-05
**
The apoptotic rate(%)
Control
50mW/cm² (5min)
P=0.0003
**
The apoptotic rate(%)
Control
50mW/cm²(10min)
P=0.0082
**
The apoptotic rate(%)
50mW/cm²(5min)
50mW/cm²(10min)
G
P=0.0083
**
The apoptotic rate(%)
25mW/cm² (5min)
50mW/cm² (5min)
P=0.0048
**
The apoptotic rate(%)
25mW/cm² (10min)
50mW/cm² (10min)

Figure 6. THz treatment-induced apoptosis of mNSCs

(A) Representative flow cytometry analysis of the mNSC apoptotic rate with 25 mW/cm^2 THz irradiation (n = 3 samples from 3 mice, 1 sample per mouse).
(B, C, and D) Quantification of the mNSC apoptotic rate in different THz treatment time groups: 25 mW/cm^2 (5 min) and 25 mW/cm^2 (10 min). ** means $p < 0.01$, * means $p < 0.05$.
(E) Representative flow cytometry analysis picture of mNSCs apoptotic rate with 50 mW/cm^2 THz irradiation (n = 3 samples from 3 mice, 1 sample per mouse).
(F) Quantification of the mNSC apoptotic rate in different THz treatment time groups: 50 mW/cm^2 (5 min) and 50 mW/cm^2 (10 min). ** means $p < 0.01$.
(G) Quantification of the mNSC apoptotic rate in different THz irradiation intensity groups: 25 mW/cm^2 (5 min) and 50 mW/cm^2 (5 min), 25 mW/cm^2 (10 min), and 50 mW/cm^2 (10 min). ** means $p < 0.01$.

In addition, a study has shown that primary hippocampal and cortical neurons are relatively sensitive to THz waves. The biological effects were positively correlated with the exposure time of the THz waves.[38] Rat glial cells exposed to THz radiation for 1 to 5 min showed a dose-dependent cytotoxic effect.[29] These studies have shown that THz irradiation can lead to changes in cellular physiological functions. However, a study to confirm whether neural stem cells exposed to THz irradiation exhibit specific biological responses has not been performed, and our study fills that gap. Furthermore, our research materials are not limited to mNSCs. We also carried out relevant experiments in hNSCs. These cell models effectively avoid the limitations of other researchers who only focus on animal models. In the course of our study, we found some differences in the response of mouse and hNSCs to THz irradiation by performing experiments with two types of neural stem cells. These suggested that it is necessary to conduct our experiments in hNSCs, which exhibit some human-specific responses to THz irradiation. The results obtained in human models are indispensable for studying the safety of THz irradiation, which will further advance the understanding of THz applications. Similar to previous studies, our results also show that THz treatment may disrupt the proliferation of NSCs and increase DNA damage and apoptosis.

For the past few years, an increasing number of studies have begun to reveal the underlying molecular mechanisms of THz irradiation leading to changes in cell physiological functions. Shang et al. showed that THz irradiation might affect the interaction between transcription factors and DNA and consequently regulate gene expression in primary neuron cells.[39] Yamazaki et al. reported that THz irradiation enhances the polymerization of purified actin *in vitro* and increases cytoplasmic F-actin *in vivo*.[40,41] Moreover, in THz-irradiated human skin cells, studies have shown explicit activation of an inflammatory response and suppression of promitotic signaling, including the suppression of cellular functions, such as cell division, differentiation, motility, and apoptosis.[42] Moreover, Kim et al. suggested that THz radiation initiates a wound-like signal in mouse skin with increased expression of TGF-β and activation of its downstream target genes, which perturbs the wound healing process *in vivo*.[43]

In summary, we found that THz irradiation alters the physiological status of neural stem cells, resulting in inhibition of proliferation and increased DNA damage and apoptosis. Furthermore, the degree of DNA damage and apoptosis of neural stem cells was proportional to the THz average output power and irradiation time. In addition, hNSCs are more vulnerable to THz irradiation than mNSCs.

Limitations of the study

In this study, we only observed the phenotypes of neural stem cells under THz irradiation without further investigation of the underlying mechanism of phenotypic changes. This issue is also a deficiency of our study, which needs to be further investigated.

STAR★METHODS

Detailed methods are provided in the online version of this paper and include the following:

- KEY RESOURCES TABLE
- RESOURCE AVAILABILITY
  - Lead contact
  - Materials availability
  - Data and code availability
- EXPERIMENTAL MODEL AND STUDY PARTICIPANT DETAILS
  - Animals
  - Mouse neural stem cells (mNSCs)
  - Human neural stem cells (hNSCs)
  - THz Generator

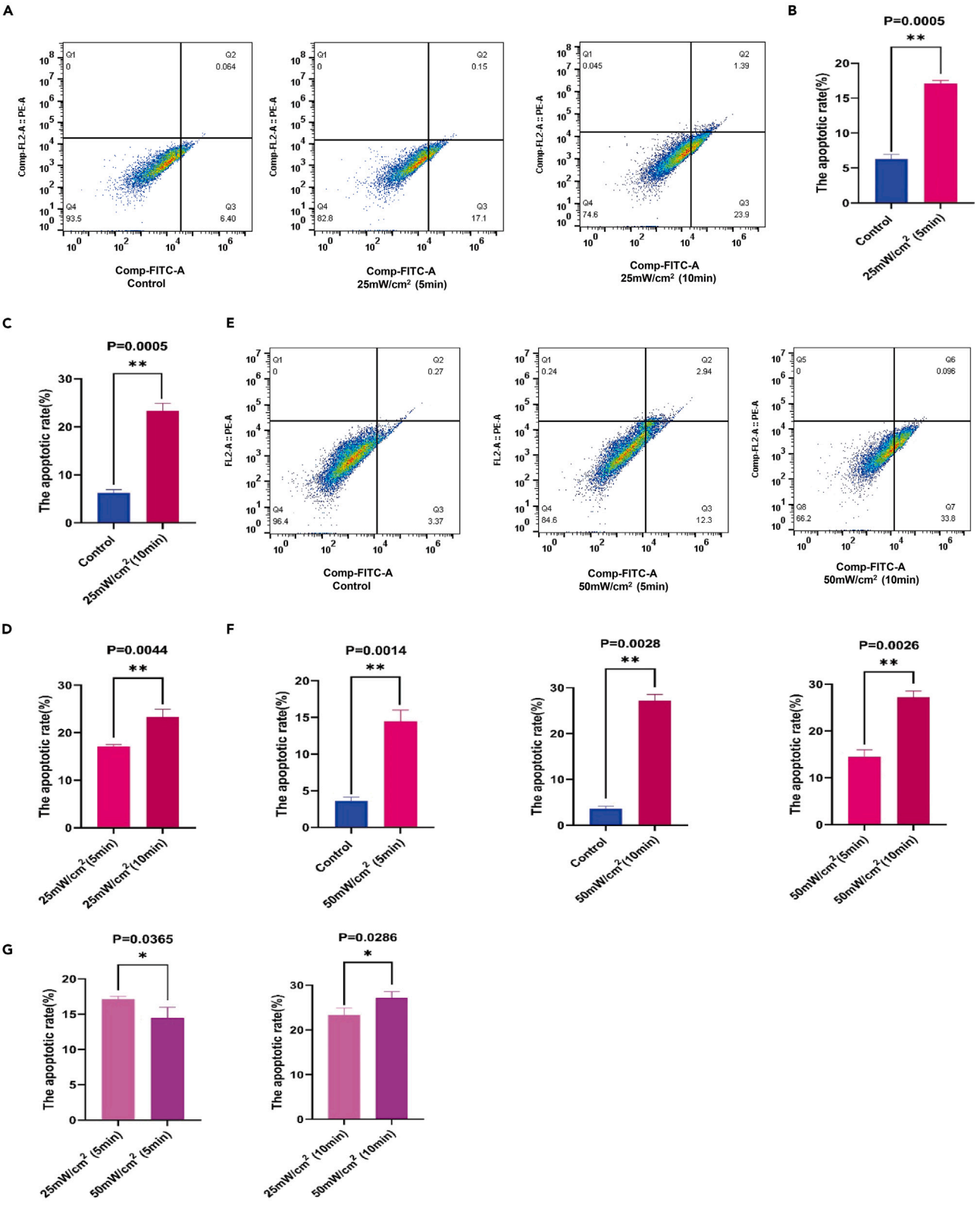
A
Q1
0
Q2
0.064
Q4
93.5
Q3
6.40
Comp-FL2-A :: PE-A
Comp-FITC-A
Control
Q1
0
Q2
0.15
Q4
82.8
Q3
17.1
Comp-FITC-A
25mW/cm² (5min)
Q1
0.045
Q2
1.39
Q4
74.6
Q3
23.9
Comp-FITC-A
25mW/cm² (10min)
B
P=0.0005
**
The apoptotic rate(%)
Control
25mW/cm² (5min)
C
P=0.0005
**
The apoptotic rate(%)
Control
25mW/cm² (10min)
E
Q1
0
Q2
0.27
Q4
96.4
Q3
3.37
FL2-A :: PE-A
Comp-FITC-A
Control
Q1
0.24
Q2
2.94
Q4
84.6
Q3
12.3
Comp-FITC-A
50mW/cm² (5min)
Q5
0
Q6
0.098
Q8
66.2
Q7
33.8
Comp-FL2-A :: PE-A
Comp-FITC-A
50mW/cm² (10min)
D
P=0.0044
**
The apoptotic rate(%)
25mW/cm² (5min)
25mW/cm² (10min)
F
P=0.0014
**
The apoptotic rate(%)
Control
50mW/cm² (5min)
P=0.0028
**
The apoptotic rate(%)
Control
50mW/cm² (10min)
P=0.0026
**
The apoptotic rate(%)
50mW/cm² (5min)
50mW/cm² (10min)
G
P=0.0365
*
The apoptotic rate(%)
25mW/cm² (5min)
50mW/cm² (5min)
P=0.0286
*
The apoptotic rate(%)
25mW/cm² (10min)
50mW/cm² (10min)

Figure 7. THz irradiation-induced apoptosis of hNSCs

(A) Representative flow cytometry analysis of the hNSC apoptotic rate with 25 mW/cm^2 THz irradiation (n = 3).

(B, C, and D) Quantification of the hNSC apoptotic rate in different THz treatment time groups: 25 mW/cm^2 (5 min) and 25 mW/cm^2 (10 min). ** means $p < 0.01$.

(E) Representative flow cytometry analysis of the hNSC apoptotic rate with 50 mW/cm^2 THz irradiation (n = 3).

(F) Quantification of the hNSC apoptotic rate in different THz treatment time groups: 50 mW/cm^2 (5 min) and 50 mW/cm^2 (10 min). ** means $p < 0.01$.

(G) Quantification of the hNSC apoptotic rate in different THz irradiation intensity groups: 25 mW/cm^2 (5 min) and 50 mW/cm^2 (5 min), 25 mW/cm^2 (10 min) and 50 mW/cm^2 (10 min). * means $p < 0.05$.

ACKNOWLEDGMENTS

We would like to thank Chunhai Chen professor for assistance in neural stem cells treatment. We thank all members of Zhang Lab for their assistance and helpful discussion on the manuscript. This work is supported by the Military Logistics Application Basic Research Project (AWS17J010), the Army Military Medical University Clinical Technology Innovation Cultivation Project (CX2019JS105), the National Natural Science Foundation of China (Grant No. 81873981), and the Chongqing Health Commission (2019ZDXM025).

AUTHOR CONTRIBUTIONS

Y.X.W. and L.Q.Z. designed the experiments and supervised the project. Y.X.W., Y.X., Q.M., P.G., and M.C. were responsible for the major experiments, and manuscript writing. H.Y.H. analyzed data. L.Q.Z., G.M.X., and F.L. revised the manuscript. All authors read and approved the final manuscript.

DECLARATION OF INTERESTS

The authors declare no competing interests.

Received: January 17, 2023
Revised: June 26, 2023
Accepted: July 14, 2023
Published: July 18, 2023

REFERENCES

1. Shumyatsky, P., and Alfano, R.R. (2011). Terahertz sources. J. Biomed. Opt. *16*, 033001. https://doi.org/10.1117/1.3554742.

2. Tao, Y.H., Fitzgerald, A.J., and Wallace, V.P. (2020). Non-Contact, Non-Destructive Testing in Various Industrial Sectors with Terahertz Technology. Sensors *20*, 712. https://doi.org/10.3390/s20030712.

3. Zhang, J., Li, S., and Le, W. (2021). Advances of terahertz technology in neuroscience: Current status and a future perspective. iScience *24*, 103548. https://doi.org/10.1016/j.isci.2021.103548.

4. Pickwell, E., and Wallace, V.P. (2006). Biomedical applications of terahertz technology. J. Phys. D Appl. Phys. *39*, R301–R310. https://doi.org/10.1088/0022-3727/39/17/R01.

5. Siegel, P.H. (2004). Terahertz technology in biology and medicine. IEEE Trans. Microw. Theory Tech. *52*, 2438–2447. https://doi.org/10.1109/TMTT.2004.835916.

6. Abufadda, M.H., Erdélyi, A., Pollák, E., Nugraha, P.S., Hebling, J., Fülöp, J.A., and Molnár, L. (2021). Terahertz pulses induce segment renewal via cell proliferation and differentiation overriding the endogenous regeneration program of the earthworm *Eisenia andrei*. Biomed. Opt Express *12*, 1947–1961. https://doi.org/10.1364/boe.416158.

7. Marble, C.B., and Yakovlev, V.V. (2020). Biomedical optics applications of advanced lasers and nonlinear optics. J. Biomed. Opt. *25*, 1–9. https://doi.org/10.1117/1.Jbo.25.4.040902.

8. Cheng, Y., Wang, Y., Niu, Y., and Zhao, Z. (2020). Concealed object enhancement using multi-polarization information for passive millimeter and terahertz wave security screening. Opt Express *28*, 6350–6366. https://doi.org/10.1364/oe.384029.

9. Yu, L., Hao, L., Meiqiong, T., Jiaoqi, H., Wei, L., Jinying, D., Xueping, C., Weiling, F., and Yang, Z. (2019). The medical application of terahertz technology in non-invasive detection of cells and tissues: opportunities and challenges. RSC Adv. *9*, 9354–9363. https://doi.org/10.1039/C8RA10605C.

10. Zhang, W., Tang, Y., Shi, A., Bao, L., Shen, Y., Shen, R., and Ye, Y. (2018). Recent Developments in Spectroscopic Techniques for the Detection of Explosives. Materials *11*. https://doi.org/10.3390/ma11081364.

11. Bychanok, D., Gorokhov, G., Plyushch, A., Ronca, A., Lavorgna, M., Xia, H., Lamberti, P., and Kuzhir, P. (2020). Terahertz Optics of Materials with Spatially Harmonically Distributed Refractive Index. Materials *13*. https://doi.org/10.3390/ma13225208.

12. Ma, Z.T., Geng, Z.X., Fan, Z.Y., Liu, J., and Chen, H.D. (2019). Modulators for Terahertz Communication: The Current State of the Art. Research6482975. https://doi.org/10.34133/2019/6482975.

13. Jasteh, D., Hoare, E.G., Cherniakov, M., and Gashinova, M. (2016). Experimental Low-Terahertz Radar Image Analysis for Automotive Terrain Sensing. IEEE Geosci. Remote Sens. Lett. *13*, 490–494. https://doi.org/10.1109/LGRS.2016.2518579.

14. Islam, M.S., Cordeiro, C.M.B., Franco, M.A.R., Sultana, J., Cruz, A.L.S., and Abbott, D. (2020). Terahertz optical fibers [Invited]. Opt

Express *28*, 16089–16117. https://doi.org/10.1364/oe.389999.

15. Zhang, L., Dong, Z., Wang, L., Hu, Y., Guo, C., Guo, L., Chen, Y., Han, L., Zhang, K., Tian, S., et al. (2021). Ultrasensitive and Self-Powered Terahertz Detection Driven by Nodal-Line Dirac Fermions and Van der Waals Architecture. Adv. Sci. *8*, e2102088. https://doi.org/10.1002/advs.202102088.

16. Zhao, L., Hao, Y.H., and Peng, R.Y. (2014). Advances in the biological effects of terahertz wave radiation. Mil. Med. Res. *1*, 26. https://doi.org/10.1186/s40779-014-0026-x.

17. Zhou, J., Zhao, X., Huang, G., Yang, X., Zhang, Y., Zhan, X., Tian, H., Xiong, Y., Wang, Y., and Fu, W. (2021). Molecule-Specific Terahertz Biosensors Based on an Aptamer Hydrogel-Functionalized Metamaterial for Sensitive Assays in Aqueous Environments. ACS Sens. *6*, 1884–1890. https://doi.org/10.1021/acssensors.1c00174.

18. Kadantsev, V.N., and Goltsov, A. (2020). Collective excitations in α-helical protein structures interacting with the water environment. Electromagn. Biol. Med. *39*, 419–432. https://doi.org/10.1080/15368378.2020.1826961.

19. Wu, K., Qi, C., Zhu, Z., Wang, C., Song, B., and Chang, C. (2020). Terahertz Wave Accelerates DNA Unwinding: A Molecular Dynamics Simulation Study. J. Phys. Chem. Lett. *11*, 7002–7008. https://doi.org/10.1021/acs.jpclett.0c01850.

20. Zhang, J., Liu, L., Chen, Y., Wang, B., Ouyang, C., Tian, Z., Gu, J., Zhang, X., He, M., Han, J., and Zhang, W. (2019). Water Dynamics in the Hydration Shell of Amphiphilic Macromolecules. J. Phys. Chem. B *123*, 2971–2977. https://doi.org/10.1021/acs.jpcb.9b02040.

21. Sun, L., Zhao, L., and Peng, R.Y. (2021). Research progress in the effects of terahertz waves on biomacromolecules. Mil. Med. Res. *8*, 28. https://doi.org/10.1186/s40779-021-00321-8.

22. Elayan, H., Eckford, A.W., and Adve, R.S. (2021). Information Rates of Controlled Protein Interactions Using Terahertz Communication. IEEE Trans. NanoBioscience *20*, 9–19. https://doi.org/10.1109/tnb.2020.3021825.

23. Sitnikov, D.S., Ilina, I.V., Revkova, V.A., Konoplyannikov, M.A., Kalsin, V.A., and Baklaushev, V.P. (2021). Cell proliferation under intense pulses of terahertz radiation. J. Phys, Conf. Ser. *1787*, 012030. https://doi.org/10.1088/1742-6596/1787/1/012030.

24. Cherkasova, O.P., Serdyukov, D.S., Ratushnyak, A.S., Nemova, E.F., Kozlov, E.N., Shidlovskii, Y.V., Zaytsev, K.I., and Tuchin, V.V. (2020). Effects of Terahertz Radiation on Living Cells: a Review. Opt. Spectrosc. *128*, 855–866. https://doi.org/10.1134/S0030400X20060041.

25. De Amicis, A., Sanctis, S.D., Cristofaro, S.D., Franchini, V., Lista, F., Regalbuto, E., Giovenale, E., Gallerano, G.P., Nenzi, P., Bei, R., et al. (2015). Biological effects of in vitro THz radiation exposure in human foetal fibroblasts. Mutat. Res. Genet. Toxicol. Environ. Mutagen. *793*, 150–160. https://doi.org/10.1016/j.mrgentox.2015.06.003.

26. Hintzsche, H., Jastrow, C., Kleine-Ostmann, T., Stopper, H., Schmid, E., and Schrader, T. (2011). Terahertz radiation induces spindle disturbances in human-hamster hybrid cells. Radiat. Res. *175*, 569–574. https://doi.org/10.1667/rr2406.1.

27. Titova, L.V., Ayesheshim, A.K., Golubov, A., Fogen, D., Rodriguez-Juarez, R., Hegmann, F.A., and Kovalchuk, O. (2013). Intense THz pulses cause H2AX phosphorylation and activate DNA damage response in human skin tissue. Biomed. Opt Express *4*, 559–568. https://doi.org/10.1364/boe.4.000559.

28. Cherkasova, O.P., Serdyukov, D.S., Nemova, E.F., Ratushnyak, A.S., Kucheryavenko, A.S., Dolganova, I.N., Xu, G., Skorobogatiy, M., Reshetov, I.V., Timashev, P.S., et al. (2021). Cellular effects of terahertz waves. J. Biomed. Opt. *26*, 090902. https://doi.org/10.1117/1.Jbo.26.9.090902.

29. Borovkova, M., Serebriakova, M., Fedorov, V., Sedykh, E., Vaks, V., Lichutin, A., Salnikova, A., and Khodzitsky, M. (2017). Investigation of terahertz radiation influence on rat glial cells. Biomed. Opt Express *8*, 273–280. https://doi.org/10.1364/boe.8.000273.

30. Wilmink, G., Rivest, B., Ibey, B., Roth, C., Bernhard, J., and Roach, W. (2010). Quantitative Investigation of the Bioeffects Associated with Terahertz Radiation. https://doi.org/10.1117/12.844916.

31. Bogomazova, A.N., Vassina, E.M., Goryachkovskaya, T.N., Popik, V.M., Sokolov, A.S., Kolchanov, N.A., Lagarkova, M.A., Kiselev, S.L., and Peltek, S.E. (2015). No DNA damage response and negligible genome-wide transcriptional changes in human embryonic stem cells exposed to terahertz radiation. Sci. Rep. *5*, 7749. https://doi.org/10.1038/srep07749.

32. Tachizaki, T., Sakaguchi, R., Terada, S., Kamei, K.I., and Hirori, H. (2020). Terahertz pulse-altered gene networks in human induced pluripotent stem cells. Opt. Lett. *45*, 6078–6081.

33. Alexandrov, B.S., Rasmussen, K.Ø., Bishop, A.R., Usheva, A., Alexandrov, L.B., Chong, S., Dagon, Y., Booshehri, L.G., Mielke, C.H., Phipps, M.L., et al. (2011). Non-thermal effects of terahertz radiation on gene expression in mouse stem cells. Biomed. Opt Express *2*, 2679–2689. https://doi.org/10.1364/boe.2.002679.

34. Bock, J., Fukuyo, Y., Kang, S., Phipps, M.L., Alexandrov, L.B., Rasmussen, K.Ø., Bishop, A.R., Rosen, E.D., Martinez, J.S., Chen, H.T., et al. (2010). Mammalian stem cells reprogramming in response to terahertz radiation. PLoS One *5*, e15806. https://doi.org/10.1371/journal.pone.0015806.

35. Qi, M., Liu, R., Li, B., Wang, S., Fan, R., Zhao, X., and Xu, D. (2022). Behavioral Effect of Terahertz Waves in C57BL/6 Mice. Biosensors *12*, 79. https://doi.org/10.3390/bios12020079.

36. Cheon, H., Yang, H.J., Choi, M., and Son, J.H. (2019). Effective demethylation of melanoma cells using terahertz radiation. Biomed. Opt Express *10*, 4931–4941. https://doi.org/10.1364/boe.10.004931.

37. Kovalevska, L., Golenkov, O., Kulahina, Y., Callender, T., Sizov, F., and Kashuba, E. (2022). A Comparative Study on the Viability of Normal and Cancerous Cells upon Irradiation with a Steady Beam of THz Rays. Life *12*. https://doi.org/10.3390/life12030376.

38. Tan, S.Z., Tan, P.C., Luo, L.Q., Chi, Y.L., Yang, Z.L., Zhao, X.L., Zhao, L., Dong, J., Zhang, J., Yao, B.W., et al. (2019). Exposure Effects of Terahertz Waves on Primary Neurons and Neuron-like Cells Under Nonthermal Conditions. Biomed. Environ. Sci. *32*, 739–754. https://doi.org/10.3967/bes2019.094.

39. Shang, S., Wu, X., Zhang, Q., Zhao, J., Hu, E., Wang, L., and Lu, X. (2021). 0.1 THz exposure affects primary hippocampus neuron gene expression via alternating transcription factor binding. Biomed. Opt Express *12*, 3729–3742. https://doi.org/10.1364/boe.426928.

40. Yamazaki, S., Harata, M., Idehara, T., Konagaya, K., Yokoyama, G., Hoshina, H., and Ogawa, Y. (2018). Actin polymerization is activated by terahertz irradiation. Sci. Rep. *8*, 9990. https://doi.org/10.1038/s41598-018-28245-9.

41. Yamazaki, S., Ueno, Y., Hosoki, R., Saito, T., Idehara, T., Yamaguchi, Y., Otani, C., Ogawa, Y., Harata, M., and Hoshina, H. (2021). THz irradiation inhibits cell division by affecting actin dynamics. PLoS One *16*, e0248381. https://doi.org/10.1371/journal.pone.0248381.

42. Hough, C.M., Purschke, D.N., Huang, C., Titova, L.V., Kovalchuk, O., Warkentin, B.J., and Hegmann, F.A. (2018). Topology-Based Prediction of Pathway Dysregulation Induced by Intense Terahertz Pulses in Human Skin Tissue Models. J. Infrared, Millim. Terahertz Waves *39*, 887–898. https://doi.org/10.1007/s10762-018-0512-4.

43. Kim, K.-T., Park, J., Jo, S.J., Jung, S., Kwon, O.S., Gallerano, G.P., Park, W.-Y., and Park, G.-S. (2013). High-power femtosecond-terahertz pulse induces a wound response in mouse skin. Sci. Rep. *3*, 2296. https://doi.org/10.1038/srep02296.

STAR★METHODS

KEY RESOURCES TABLE

REAGENT or RESOURCE	SOURCE	IDENTIFIER
Antibodies		
Cy3-labeled Goat Anti-Rabbit IgG (H + L)	Beyotime	A0516; RRID: AB_2893015
Anti-γH2A.X	Abcam	ab81299; RRID: AB_1640564
Chemicals, peptides, and recombinant proteins		
rhbFGF	Stem Cell	78003
heparin solution	Stem Cell	07980
neurobasal medium	Gibco	12348–017
mouse EGF	Gibco	PMG8041
B-27 supplement (50×)	Gibco	12587–010
penicillin/streptomycin	Gibco	15140–122
4% paraformaldehyde solution	Beyotime	P0099
QuickBlock™ buffer	Beyotime	P0252
4′,6-diamidino-2-phenylindole (DAPI)	Beyotime	C1005
Accutase	Sigma Technology	A6964
NeuroCult™ NS-A Basal Medium	Human	Cat#05750
NeuroCult™ NS-A Proliferation Supplement	Human	Cat#05753
Critical commercial assays		
Proliferation detection kits	BeyoClick™ EdU-488	C0071
Apoptotic detection kits	Beyotime	C1062M
Experimental models: Cell lines		
hNSCs (Human neural stem cell)	Induced from iPS cell line using cellapy's method	Cellapy (support@cellapybio.com
mNSCs (Mouse neural stem cell)	Isolated from newborn C57BL/6 mice	Cyagen (https://www.cyagen.com/cn/zh-cn/community.htmL)
iPS cell line	Boston Children's Hospital	Coriell #GM23338; RRID: CVCL_F182
Software and algorithms		
ImageJ 1.53a software	ImageJ	https://imagej.net/downloads
FlowJo 10.3	FlowJo™ Software (BD Biosciences)	https://www.bdbiosciences.com/en-us/products/software/flowjo-v10-software
Graphpad Prism 9.0.0	GraphPad	https://www.graphpad.com/
Other		
Leica DMI8 fluorescence microscope	Leica	Leica DMI8
BD Accuri C6 plus flow cytometer	BD	BD Accuri C6 plus

RESOURCE AVAILABILITY

Lead contact

Further information and requests for resources and reagents should be directed to and will be fulfilled by the lead contact, Liqun Zhang (1434103777@qq.com).

Materials availability

This study did not generate any new materials.

Data and code availability

- All data reported in this paper will be shared by the lead contact upon request.
- This paper does not report the original code.
- Any additional information required to reanalyze the data reported in this paper is available from the lead contact upon request.

EXPERIMENTAL MODEL AND STUDY PARTICIPANT DETAILS

Animals

The mice used in the experiments were wild-type C57BL/6. Three-month-old female mice and male mice were housed in the specific pathogen-free (SPF) animal facility. One male mouse was paired with per two females to produce offspring, and the mice had freely available water and food. All mice were maintained in a constant temperature environment with a regular diurnal lighting cycle (12 h–12 h light and dark cycle). Finally, newborn mice were used to isolate neural stem cells. In the experiment, we only used neural stem cells isolated from newborn mice. Therefore, gender differences had no effect on the experimental results. The assays were performed at least three times. All animal experiments were performed by following the Laboratory Animal Welfare and Ethics Committee of the Army Medical University guidelines.

Mouse neural stem cells (mNSCs)

First, the head of newborn mice was stripped of the skull，and the brain tissue was washed three times in D-PBS (Dulbecco's phosphate buffered saline) containing penicillin/streptomycin (1:500). At the end of the washing, brain tissue was placed into a 1.5 mL EP tube, cut into pieces and digested with 1 mL of Accutase digestive enzyme for 15 min, and the mixture was reversed every 5 min to promote brain tissue digestion. After digestion, the mixture was centrifuged for 3 min (3000 rpm/min), the upper layer of the digest was removed, and neural stem cell medium was added and mixed thoroughly. Then, the mixture was transferred to a 10-cm culture dish and supplemented with neural stem cell medium to 8 mL. These mNSCs were maintained at 37°C with 5% CO_2 in the cell incubator for five days, and the medium was replaced every three days. On the sixth day, single neural stem cells were transferred to a six-well plate for adherent culture and further experiments. After the addition of the medium, the depth of the culture fluid above the stem cells was 2 mm. The neural stem cell medium contained rhbFGF (Stem Cell, 78003), neurobasal medium (Gibco, 12348-017), mouse EGF (Gibco, PMG8041), heparin solution (Stem Cell, 07980), B-27 supplement (50x) (Gibco, 12587-010) and penicillin/streptomycin. (Gibco, 15140-122).

Human neural stem cells (hNSCs)

The iPS cell line was obtained from Harvard Medical School. First, these cells were plated on a six-well plate coated with 0.1% gelatin to promote cell reproduction. Then, human iPSCs were induced into hNSCs using the protocol from Cellapy (support@cellapybio.com). After the induced pluripotent stem cells were grown to 100% confluency in a six-well plate, the human neural stem cell induction medium was removed from the refrigerator and brought to room temperature. Then, the iPSC medium was removed, the cells were washed with D-PBS three times, and neural stem cell induction medium was added to the six-well plate. iPSCs were cultured in a constant temperature cell incubator with a temperature of 37°C and 5% CO_2. The induction medium was completely changed every 48 h, and the human neural stem cell induction medium (6 mL/well) was changed every time. For the differentiation of neural stem cells, iPSCs were cultured for six days using a neural induction medium. A large number of scattered rosettes appear under the microscope, and the induction period has passed. After that, these hNSCs were cultured in NeuroCult NS-A Basal Medium (Human) (Cat#05750) including heparin solution (Stem Cell, 07980), NeuroCult NS-A Proliferation Supplement (Human) (Cat#05753), rhbFGF (Stem Cell, 78003) and EGF (Gibco, PMG8041). After the addition of the medium, the depth of the culture fluid above the stem cells was 2 mm. Finally, these neural stem cells were cultured for three days to ensure that the number of cells was sufficient for the relevant experiments.

THz Generator

The THz radiation installation (Figure 1) is mainly composed of a 0.22 THz line wave tube, front solid signal source, high voltage source, cold cooling system, test, test components and control system composition. For the device, the production center frequency is 0.22 THz, and the output work rate is up to 1.18 W THz

wave beam. The six-well plate was removed from the cell incubator, and the culture dish was placed on the target platform under the THz transmission system. The THz wave was taken from the upper part of the fine cellular orifice plate, and the temperature of the fine cell culture base in the THz radiation path was controlled at the same time at 25°C. Due to the absorption of terahertz waves by water in the cell culture medium, when cells are irradiated, the culture medium in the cell culture plate only covers the cells to maintain their normal growth state, which minimizes the absorption of terahertz waves by water in the culture medium. In the radiation passage, a thermoelectric couple thermometer was used for real-time monitoring of cell culture medium temperature changes. The neural stem cell experiments of different species were divided into five groups: control group, 25 mW/cm^2 (5 min) irradiation group, 25 mW/cm^2 (10 min) irradiation group, 50 mW/cm^2 (5 min) irradiation group, and 50 mW/cm^2 (10 min) irradiation group. Controls consisted of identical cell plates and conditions but were not irradiated. Finally, cell proliferation, DNA damage, and apoptosis were detected at 24 h or 48 h in different treatment groups after the same THz irradiation.

METHOD DETAILS

Flow cytometry analysis

Proliferation detection kits (BeyoClick EdU-488, C0071) were used to detect the proliferation of neural stem cells. First, the balls of cells were dissociated into single cells, and then, the digested single cells were cultured in a suspension medium for 2 h after adding EdU. Next, at least three million cells were obtained with 75% ethanol treatment at 4°C overnight. After that, these cells were washed three times with cold D-PBS. After three washes, the cells were treated according to the protocol provided by Beyotime (https://www.beyotime.com/product/C0071S.htm). After EdU treatment, remove the medium and add 1 mL fixative solution (Beyond 4% paraformaldehyde P0099). Then, fix the cell at room temperature for 15 min. After that, remove the 4% paraformaldehyde, and wash the cells with 1 mL washing solution for each well 3 times, 3–5 min each time. Next, the Click Additive Solution was prepared, add 0.5 mL Click Additive Solution to each well and incubate the cells at room temperature for 30 min in the dark. Finally, the Click Additive Solution was aspirated and washed 3 times with D-PBS. Cell proliferation were analyzed by a BD Accuri C6 plus flow cytometer three times.

The NSCs were dissociated into single cells by Accutase (Sigma Technology, USA, A6964), and then, the cells were treated with 4% paraformaldehyde solution (Beyotime, P0099) for approximately 30 min. After that, these cells were treated with fixation/permeabilization buffer for 1 h at 4°C and incubated with anti-γH2A. X diluted antibody (Abcam; ab81299) for 2 h. Then, the cells were treated with secondary antibodies in the dark and washed in D-PBS three times. Finally, a BD Accuri C6 plus flow cytometer was used to analyze these cells and detect the proportion of DNA-damaged cells.

Immunofluorescence assay

First, the neural stem cells were digested and plated on a 12-well plate at a density of half a million cells per well. After 48 h of incubation in the incubator, these cells were fixed with 4% paraformaldehyde for 15 min. After that, the samples were washed three times with PBST (phosphate-buffered saline, 0.1% Triton X-100) for 5 min each time. After the cells were treated with QuickBlock buffer (Beyotime, P0252) for 30 min at room temperature, the cells were incubated with primary antibodies (anti-γH2A.X, Abcam; ab81299) overnight at 4°C. After incubation with the primary antibodies, the cells were washed three times with cold D-PBS and then reacted with the secondary antibodies (1:1000 dilution in blocking buffer) for 2 h in the dark. Finally, these cells were treated with 4′,6-diamidino-2-phenylindole (DAPI) (Beyotime, C1005) for 10 min and washed with D-PBS three times. The coverslips were enclosed on histological slides with glycerol. The images were collected with a Leica DMI8 fluorescence microscope (Wetzlar, Germany). ImageJ software was used to analyze and quantify the image differences, including fluorescence intensity and the proportion of γH2A.X. The selection area was the same in the images of different treatment groups, and at least three biologically independent experiments were performed after subtracting the background. The results are shown as the mean ± SEM. p values were calculated by the two-tailed samples paired t test.

QUANTIFICATION AND STATISTICAL ANALYSIS

All data are represented as mean ± SD, with 95% confidence intervals. Statistical evaluations of cell proliferation and apoptosis were conducted using two-tail unpaired Student's *t* test (data with normal

distribution) for comparison of two independent groups in FCM experiments. n = three biologically independent experiments. Statistical analyses of DNA damage were conducted using two-tail unpaired Student's *t* test (data with normal distribution) for comparison of two independent groups in immunofluorescence experiments. n = three biologically independent experiments. A critical value of $p < 0.05$ was set for statistical significance throughout the study. All data were performed using Graphpad Prism 9.0.0 software unless otherwise noted.